

COMPAS: Representation Learning with Compositional Part Sharing for Few-Shot Classification

Ju He Adam Kortylewski Alan Yuille
Johns Hopkins University

Abstract

Few-shot image classification consists of two consecutive learning processes: 1) In the meta-learning stage, the model acquires a knowledge base from a set of training classes. 2) During meta-testing, the acquired knowledge is used to recognize unseen classes from very few examples. Inspired by the compositional representation of objects in humans, we train a neural network architecture that explicitly represents objects as a set of parts and their spatial composition. In particular, during meta-learning, we train a knowledge base that consists of a dictionary of part representations and a dictionary of part activation maps that encode common spatial activation patterns of parts. The elements of both dictionaries are shared among the training classes. During meta-testing, the representation of unseen classes is learned using the part representations and the part activation maps from the knowledge base. Finally, an attention mechanism is used to strengthen those parts that are most important for each category. We demonstrate the value of our compositional learning framework for a few-shot classification using miniImageNet, tieredImageNet, CIFAR-FS, and FC100, where we achieve state-of-the-art performance.

1. Introduction

Advances in the architecture design of deep convolutional neural networks (DCNNs) [17, 31, 11] increased the performance of computer vision systems at image classification enormously. However, in practice, their performance is usually limited when not enough labeled data is available. Few-shot classification is concerned with the problem of learning from a small number of samples. In particular, it consists of two consecutive learning processes: 1) In the meta-learning stage, the model acquires a knowledge base from a set of training classes. 2) During meta-testing, the acquired knowledge is used to recognize unseen classes from very few examples. Hence, few-shot classification wants to emulate human learning efficiency by requiring to transfer the knowledge gained through training

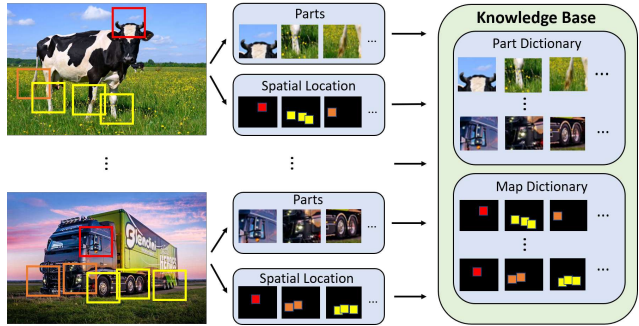


Figure 1. Intuitive illustration of how our model acquires knowledge during meta-learning. In particular, it learns a dictionary of part representations, which resemble individual object parts. Some of these can be shared across different classes, such as, e.g., car tires. In addition, it learns a map dictionary that contains common spatial activation patterns of parts. During meta-testing, the knowledge base facilitates the learning of novel classes by re-using the already learned parts and spatial activation patterns.

on a large number of base classes to enhance the learning of new classes from just a few classes.

Various approaches to few-shot classification were proposed in the past that take different perspectives on the same problem: 1) Metric-based methods aim to learn a task-invariant metric [36, 32, 34, 24]. 2) Meta-learning methods approach the problem from the perspective of learning to learn. They aim to design deep models such that the model parameters can be adapted to include new classes by optimizing very few gradient steps on a small set of new data [7, 23, 18, 39]. 3) Large-corpus-based methods directly train a model on a large base training dataset through a proxy task to get a strong and discriminative representation [8, 10, 26, 9, 35]. While these methods all try to share the common knowledge among base classes and novel classes, they do not explicitly consider that objects can have similar parts and shapes that can be reused.

In this paper, we introduce a novel approach to few-shot classification that explicitly exploits that object parts and their spatial activation patterns can be shared among different object classes. For example, the spatial structure of the class "horse" can be used for learning efficiently about the

class "donkey". We implement such a compositional part sharing by train a knowledge base during meta-learning that consists of a dictionary of part representations and a dictionary of part activation maps that encode common spatial activation patterns of parts (Figure 1). We start by extracting the feature representations of an image up to the last convolution layer of a standard backbone architecture, such as ResNet [11]. Following recent work on unsupervised part detection [19, 41, 42], the part dictionary is learned by clustering the individual feature vectors from the feature encoding of the training images. Moreover, we extract *part activation maps* by computing the spatial activation pattern of parts in the training images. The part activation maps are clustered to learn a dictionary of prototypical maps that encode the most common spatial activation patterns of parts. In practice, the elements of the map dictionary are optimized to be distinct from each other to avoid redundancies. During meta-testing, our model learns representations of objects by composing them from the parts and part activation maps of the knowledge base. We use an attention layer to increase the weight of the parts that are most discriminative for an object class. Finally, the learned object representations are fed into a classifier to predict the class label. During meta-training, the full model pipeline is trained end-to-end. During meta-testing, we observed that it is sufficient to train the classification head only, while freezing the learned backbone and knowledge base. This is different from the majority of other meta-learning methods and highlights the strong generalization performance induced by integrating compositional part sharing into neural networks.

We evaluate our model on four popular few-shot classification datasets (miniImageNet [36], tieredImageNet [29], CIFAR-FS [1], Fewshot-CIFAR100 [24]) and achieve state-of-the-art performance on all datasets. In summary, we make several important contributions in this work:

1. To the best of our knowledge, we are the first to study and demonstrate the effectiveness of compositional part sharing on few-shot classification.
2. We introduce COMPAS, a novel neural architecture for few-shot classification that implements the inductive prior of compositional part sharing. It learns a knowledge base with part representations and their common spatial activation patterns, and re-uses this knowledge to learn efficiently about novel classes.
3. We achieve SOTA performance on several standard benchmarks, outperforming many recent complex optimization methods.

2. Related Work

In this section, we review existing work on few-shot classification and compositional models.

2.1. Few-shot learning

Few-shot learning has received a lot of attention over the last years. Related work can be roughly classified into three branches: Metric-based, optimization-based, and large-corpus-based learning frameworks. We will briefly review all three of them in the following.

The core idea in metric-based few-shot learning work is related to nearest neighbor algorithms and kernel density estimation. These methods embed input data into a fixed embedding space and use these to design proper kernel functions. Matching Networks [36] employed two networks for support and query samples, respectively, followed by an LSTM with read-attention to encode the full embedding. The prototypical network [32] was designed to compare the query with class prototypes in the support set by using the euclidean distance to prototype representations. Relation Networks [34] leveraged relational module to learn the metric by the network used for evaluating distance instead of manually designed. TADAM [24] proposed metric scaling and metric task conditioning to further boost the performance of Prototypical Networks.

Another branch of methods is optimization-based. Since traditional deep learning models are not designed to train with very few samples, these methods aim to find a good initialization point or update path that can lead to a quick convergence. MAML [7] proposed a general optimization algorithm that can get big improvements on a new task with a small number of gradient steps. Reptile [23] simplified MAML by removing the re-initialization for each task. MetaOptNet [18] replaced the linear predictor with an SVM in a MAML framework and introduced a differentiable quadratic programming solver to allow end-to-end training. FEAT [39] proposed set-to-set functions for a quick adaptation from instance embeddings to the target embeddings.

While many metric-based and optimization-based works tend to solve the problem in a meta-learning way, works on large-training-corpus methods argue that training a base network on the whole training set directly is also feasible. These methods can provide stronger feature representations, thus making the model more discriminative even with few samples. Dynamic Few-shot [9] extended object recognition systems with an attention weight generator and redesigned the classifier module as the cosine similarity function. Qiao et al. [26] proposed to adapt the parameters trained on meta-training sets to meta-testing sets by predicting parameters from activations. Recently, RFS [35] showed that simply training the embedding function on the combined meta-training sets followed by knowledge distillation further improves the performance. It proves that learning a good representation through a proxy task, such as image classification, can give state-of-the-art performances.

Though all these methods improve few-shot learning in

different ways, they do not explicitly take into account that objects can have similar parts and shapes which can be reused. The work closest related to ours is the Attentive prototype [37], which introduced capsule networks to account for the lack of part representations in standard deep networks. However, they do not explicitly exploit part information, and their performance is limited by the fact that capsule networks are not robust to background noise.

2.2. Compositional part-based models

A rich literature on compositional part-based models for image classification exists. However, with the exception of very few works [6, 43], most methods use part annotations for training and do not share parts among object classes. Moreover, many traditional works [6, 43, 2, 5, 38, 44] learn the model parameters directly from image pixels. The major challenge for these approaches is that they need to explicitly account for nuisances such as illumination and deformation. Several recent works proposed to learn compositional part-based models from the features of higher layers of deep convolutional neural networks, since these features have shown to be robust to nuisances and have some semantic meanings.

Liao et al. [19] proposed to integrate compositionality into DCNNs by regularizing the feature representations of DCNNs to cluster during learning. Their qualitative results show that the resulting feature clusters resemble detectors of different parts. Zhang et al. [41] demonstrated that part detectors emerge in DCNNs by restricting the activations in feature maps to have a localized spatial distribution. Kortylewski et al. [16] proposed to learn generative dictionary-based compositional models from the features of a DCNN. They use their compositional model as “backup” to an independently trained DCNN if the DCNNs classification score falls below a certain threshold. In follow-up work, Kortylewski et al. [14, 15] further proposed a fully differentiable compositional model for image classification that shows strong robustness to either synthetic occlusion or real occlusion scenes. Sun et al. [33] demonstrated that these methods could be extended to combine image classification and amodal segmentation by leveraging compositional shape priors.

These recent advances inspire our work in integrating compositional models and deep neural networks. In particular, our model for few-shot classification learns part representations and how to compose them together spatially into a whole object representation. We exploit that parts and their spatial activation patterns can be shared among different classes, which enables our model to learn efficiently from very few examples.

3. Method

We briefly review the framework of few-shot classification in section 3.1. We present how we learn the part dic-

tionary module in section 3.2, followed by a discussion on how to learn the map dictionary module and how to integrate these modules into a pipeline for few-shot classification in section 3.3. We discuss how to train our model in an end-to-end manner in section 3.4.

3.1. Few-Shot Classification

Few-shot image classification consists of two consecutive learning processes: 1) In the meta-learning stage, the model acquires a knowledge base from a set of training classes. 2) During meta-testing, the acquired knowledge is used to recognize unseen classes from very few examples. During meta-training, a meta-task is represented as a N -way- K -shot classification problem. In this meta-task a training set is sampled with N classes and K example images per class $\mathbf{I}^{train} = \{I_1^1, \dots, I_N^K; y_1^1, \dots, y_N^K\}$. This training set is often also referred to as the support set. Moreover, a test set is sampled with additional M test images of each of the N classes, such that $\mathbf{I}^{test} = \{I_1^1, \dots, I_N^M; y_1^1, \dots, y_N^M\}$. The test set is also referred to as the query set. For meta-learning a collection of G meta-training tasks $T = \{(\mathbf{I}_g^{train}, \mathbf{I}_g^{test})\}_{g=1}^G$ is sampled, where each tuple $(\mathbf{I}_i^{train}, \mathbf{I}_i^{test})$ describes the support and query sets of the corresponding meta-task. After meta-training, the performance of the model is evaluated on meta-testing set $S = \{(\mathbf{I}_j^{train}, \mathbf{I}_j^{test})\}_{j=1}^J$ for a different set of object classes with the same numbers of samples in the support and query sets. In this paper, we follow the common setup of training our model on the combined meta-training set T . After our model is trained, we directly test on meta-testing set S without fine-tuning the model parameters.

3.2. Learning a part dictionary via clustering

Formulation. We denote a feature map $F^l \in \mathbb{R}^{H \times W \times C}$ as the output of a layer l in a deep convolutional neural network, with C being the number of channels. A feature vector $f_p^l \in \mathbb{R}^C$ is the vector of features in F^l at position p on the 2D lattice \mathcal{P} of the feature map. In the remainder of this section, we omit the superscript l for notational clarity because this is fixed a-priori.

Learning part representations. A number of prior works [19, 41, 16, 14] on learning compositional representations showed that when clustering feature vectors f_p , the cluster centers resemble image patterns that frequently occur in the training images. These patterns often share semantic meanings and therefore resemble part-like detectors. Motivated by these results, we aim at constructing a *part dictionary* $D = \{d_1, \dots, d_B\}$, in which the components $d_b \in \mathbb{R}^C$ are cluster centers of the feature vectors f_p from the training images. To achieve this, we integrate an additional clustering loss into the overall loss function when training the network (see Section 3.4 for details). Intuitively, this will encourage the dictionary components d_b

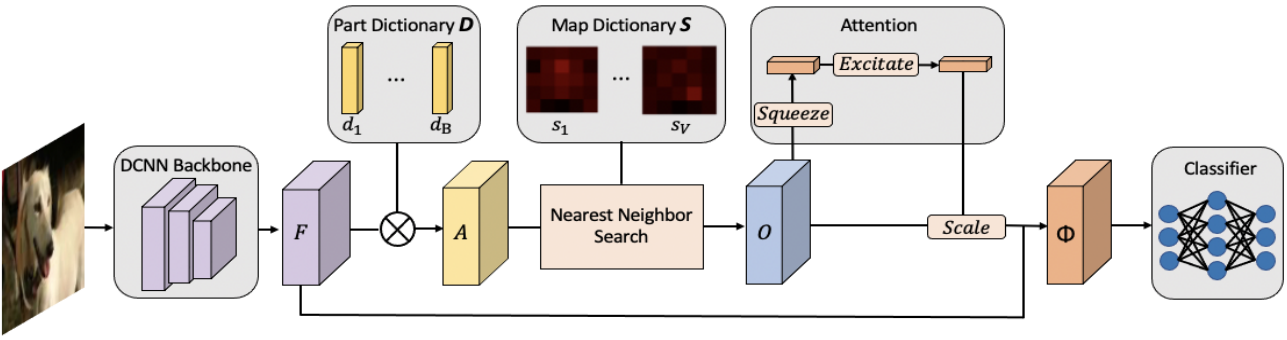


Figure 2. Feed-forward inference with COMPAS. A DCNN backbone is used to extract the feature map F . The components of the part dictionary D are used as kernels to compute a part activation map A . We then compare each channel in the part activation map A_b to the spatial patterns in the map dictionary S and multiply it element-wise with the most similar one to compute the output O . An attention mechanism is used to further strengthen parts that are most discriminative for an object class. The attention-weighted output is denoted as Φ . We concatenate Φ with average-pooled F and forward it to the classifier module to compute the final classification result.

to learn part representations from the intermediate layer l of a DCNN, and hence to capture the mid-level semantics of objects. Figure 3 illustrates examples of the dictionary components d_b after the meta-learning stage by showing image patches that activate each component the most. Note how the part representations indeed respond to semantically meaningful image patterns, such as the head of a dog.

3.3. Compositional Part Sharing for Few-Shot Classification

Computing the spatial activation maps of parts. Given the part dictionary D , we compute the activation of a part representation d_b at a position p in the feature map F by computing the cosine similarity between d_b and the feature vector f_p . We implement this module as a convolution layer, which we call *part detection layer*. The convolutional kernels of the part detection layer are the components of the part dictionary D , and their kernel size is 1×1 . At every forward time, the kernels and input feature maps are $L2$ -normalized before computing the cosine similarity. The output of part the detection layer is a part activation tensor $A \in \mathbb{R}^{H \times W \times B}$, where B is the number of components in dictionary D . Each channel in this tensor $A_b \in \mathbb{R}^{H \times W}$ is referred to as *part activation map*.

Learning dictionaries of spatial activation patterns. Our goal is to enable the model to share part activation patterns among different classes. This is inspired by the idea that parts of different objects can have similar spatial activation patterns and that this natural redundancy should be exploited (e.g. the spatial structure of the class "dog" can be used for learning efficiently about the class "wolf"). We achieve this by learning a *map dictionary* $S = \{S_1, \dots, S_V\}$, which contains the most common part activation patterns in the training data. We integrate the dictionary components $S_v \in \mathbb{R}^{H \times W}$ into the feed-forward stage by com-

paring them to the individual part activation maps A_b using the cosine similarity. We then select the closest component $\bar{v} = \arg \min_v \cos(S_v, A_b)$ and compute the output channel as point-wise multiplication between A_b and $S_{\bar{v}}$. After repeating this operation for all spatial distribution maps, we get the activated spatial distribution output denoted as $O \in \mathbb{R}^{H \times W \times B}$. In this way, each part activation map A_b is encouraged to learn information from the most similar stored spatial activation pattern S_v .

Re-weighting important parts with attention. To further augment parts that are most important for representing a particular object, we adopt an attention mechanism to calculate different weights and the relationship between the parts' spatial distributions. We follow the design of SENet [12] with small changes. In particular, we first squeeze the global spatial information of O into a channel descriptor by using a learned filter $R \in \mathbb{R}^{H \times W \times B}$. Formally, a summary vector $z \in \mathbb{R}^B$ is generated by shrinking O through its spatial dimensions $H \times W$, such that the b -th entry of the vector z is calculated by:

$$z_b = \sum_{h=1}^H \sum_{w=1}^W R_b(h, w) O_b(h, w) \in \mathbb{R}. \quad (1)$$

To fully exploit the squeezed information, we then use the same gating mechanism as SENet which contains a bottleneck with two fully-connected layers and non-linearity activation. It can be represented as

$$l = \sigma(W_2 \delta(W_1 z)) \in \mathbb{R}^B \quad (2)$$

where σ refers to the Sigmoid activation and W_1, W_2 are the weights of the fully-connected layers. With the computed activation l , the final output is obtained by re-weighting the input O with l :

$$\Phi_b = l_b \cdot O_b \in \mathbb{R}^{H \times W} \quad (3)$$

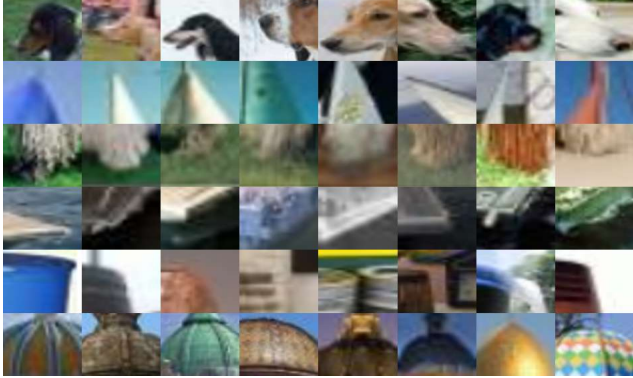


Figure 3. Illustration of the interpretability of our elements in the part dictionary. Each row visualizes image patterns from the mini-ImageNet dataset that activate a dictionary component the most.

where \cdot refers to channel-wise multiplication between the scalar l_b and the channel output O_b . Finally, we normalize feature vectors along the channel dimension in Φ to have unit norm and concatenate it with average-pooled F then forward it into the classifier to obtain a final prediction.

3.4. End-to-end Training of the model

During training, we use a two-layer fully-connected structure as a classifier to predict the classification results. Our model is fully differentiable and can be trained end-to-end using back-propagation. The trainable parameters of our model are $\Theta = \{\Omega, D, S\}$, where Ω are the parameters of the backbone used for feature extraction, e.g., ResNet-12. D is the part dictionary, and S is the dictionary of part activation maps. We optimize these parameters jointly using stochastic gradient descent. Our loss function contains three terms:

$$\mathcal{L}(y, y') = \mathcal{L}_{class}(y, y') + \gamma_1 \mathcal{L}_{cluster}(D) + \gamma_2 \mathcal{L}_{sparse}(S) \quad (4)$$

$\mathcal{L}_{class}(y, y')$ is the cross-entropy loss between the predicted label y' and the ground-truth label y . The second term $\mathcal{L}_{cluster}(D)$ is used to add additional regularization for the dictionary of parts:

$$\mathcal{L}_{cluster}(D) = \sum_p \min_b (1 - \cos(D_b | f_p)) \quad (5)$$

where f_p refers to the feature vector at position p in the feature map F and $\cos(\cdot, \cdot)$ refers to the cosine similarity. Intuitively, this loss encourages the dictionary's components to become similar to the feature vectors f_p . Thus the dictionary is forced to learn part representations that frequently occur in the training data.

To regularize the map dictionary, we add a sparse loss on

the dictionary S :

$$\mathcal{L}_{sparse} = \sum_{v=1}^V \arg \max_{v'} \cos(S_v, S_{v'})^2 \quad (6)$$

where $\cos(S_v, S_{v'})$ is the cosine similarity between two dictionary elements of S . This regularizer encourages the map dictionary elements to be sparse, thus avoiding that the elements become too similar to each other. We find that exploiting the second-order information of the cosine similarity avoids that the sparse loss will dominate the direction of the gradient at later stages of the training and thus helps the model to converge.

3.5. Replacing the classifier during meta-testing

What differs our approach from many other existed models is that we do not further fine-tune our model based on the support sets D_j^{train} in the meta-testing stage. Instead, we replace the fully-connected classification head with simpler classifier to avoid overfitting. We tested different classifier, such as nearest neighbor based on the cosine distance, the euclidean distance, and several linear classifiers such as logistic regression and a linear support vector machine. We found that the logistic regression gives the best results. In summary, for a task $(D_j^{train}, D_j^{test})$ sampled from meta-testing set S , we forward D_j^{train} through the whole embedding function to get the attentioned part activation map Φ contacted with the average-pooled F , and train the logistic regression classifier on this representation.

4. Experiment

In this section, we conduct extensive experiments that prove the effectiveness of our model. We first describe our detailed setup in section 4.1, which includes datasets, model structure, and hyper-parameters. Then we evaluate our model and make comparisons to related work on four few-shot classification benchmark datasets: miniImageNet [36], tieredImageNet [29], CIFAR-FS [1], Fewshot-CIFAR100 (FC100) [24]. The concrete performance on ImageNet derivatives is discussed in Section 4.2 and that on CIFAR derivatives is discussed in Section 4.3. We further conduct ablation studies in Section 4.4 to study the effects of the individual modules in our COMPAS pipeline.

4.1. Experimental Setups

Architecture. Following previous work [21, 24, 18, 28, 3], we use a ResNet12 as our feature extraction network which contains 4 residual blocks, where each of them contains 3 convolution layers. We drop the last average-pooling layer and use feature maps before the pooling for later computation. Dropblock is used in our model as a regularizer. We set the number of components in the part dictionary D

Table 1. **Comparison to prior work on miniImageNet and tieredImageNet.** Average few-shot classification accuracies(%) with 95% confidence intervals on the meta-testing sets of miniImageNet and tieredImageNet. a-b-c-d denotes a 4-layer convolutional network with a, b, c, d filters in each layer.

model	backbone	miniImageNet 5-way		tieredImageNet 5-way	
		1-shot	5-shot	1-shot	5-shot
MAML [7]	32-32-32-32	48.70 \pm 1.84	63.11 \pm 0.92	51.67 \pm 1.81	70.30 \pm 1.75
Matching Networks [36]	64-64-64-64	43.56 \pm 0.84	55.31 \pm 0.73	-	-
Prototypical Networks [32]	64-64-64-64	49.42 \pm 0.78	68.20 \pm 0.66	53.31 \pm 0.89	72.69 \pm 0.74
Dynamic Few-shot [9]	64-64-128-128	56.20 \pm 0.86	73.00 \pm 0.64	-	-
Relation Networks [34]	64-96-128-256	50.44 \pm 0.82	65.32 \pm 0.70	54.48 \pm 0.93	71.32 \pm 0.78
R2D2 [1]	96-192-384-512	51.2 \pm 0.6	68.8 \pm 0.1	-	-
Shot-Free [28]	ResNet-12	59.04 \pm n/a	77.64 \pm n/a	63.52 \pm n/a	82.59 \pm n/a
TEWAM [25]	ResNet-12	60.07 \pm n/a	75.90 \pm n/a	-	-
AdaResNet[22]	ResNet-12	56.88 \pm 0.62	71.94 \pm 0.57	-	-
TDADM [24]	ResNet-12	58.50 \pm 0.30	76.70 \pm 0.30	-	-
Robust 20 [4]	ResNet-12	59.38 \pm 0.65	76.90 \pm 0.42	-	-
Variational FSL [40]	ResNet-12	61.23 \pm 0.26	77.69 \pm 0.17	-	-
LEO-trainval [30]	WRN-28-10	61.76 \pm 0.08	77.59 \pm 0.12	66.33 \pm 0.05	81.44 \pm 0.09
MetaOptNet [18]	ResNet-12	62.64 \pm 0.61	78.63 \pm 0.46	65.99 \pm 0.72	81.56 \pm 0.53
FEAT [39]	WRN-28-10	65.10 \pm 0.20	81.11 \pm 0.14	70.41 \pm 0.23	84.38 \pm 0.16
RFS [35]	ResNet-12	64.82 \pm 0.60	82.14 \pm 0.43	71.52 \pm 0.69	86.03 \pm 0.49
Neg-Cosine [20]	ResNet-12	63.85 \pm 0.81	81.57 \pm 0.56	-	-
MABAS [13]	ResNet-12	65.08 \pm 0.86	82.70 \pm 0.54	74.40 \pm 0.68	86.61 \pm 0.59
Ours	ResNet-12	65.74 \pm 0.53	83.03 \pm 0.33	73.82 \pm 0.58	86.76 \pm 0.52

to 512 and the number of components in the map dictionary S to 2048 in our experiments.

Implementation details. The loss coefficients in Eq. 4 are set to $\gamma_1 = 1$ and $\gamma_2 = 0.5$ respectively. We use the SGD optimizer with a momentum of 0.9 and a weight decay of $5e^{-4}$. Our batch size is set to 64, and the base learning rate is 0.05. We initialize the part dictionary D via K-means clustering on the feature vectors f_p and fine-tune it at the meta-training stage. We found that a random initialization of the part dictionary would not reduce the final performance, but the K-means initialization helps our model to converge faster as the cluster loss is lower at the start of training. On miniImageNet and tieredImageNet, we train our model 100 epochs and for CIFAR derivatives, the total epochs for training are 90. We adopt cosine annealing as the learning rate scheduler. During training, we adopt regular data augmentation schemes such as random flipping, color jittering. When handling CIFAR derivatives datasets, we resize the input image to 84×84 pixels in order to have enough spatial resolution. Following common experimental setups, we report our performance based on an average of 600 meta-tasks, where each of them contains 15 test instances per class. For fair comparison, we only train our model on the training set of each dataset and do not perform any test-time training.

4.2. Experiments on ImageNet derivatives

The **miniImageNet dataset** is the most classic few-shot classification benchmark proposed by Matching Networks

[36]. It consists of 100 randomly sampled different classes, and each class contains 600 images of size 84×84 pixels. We follow the widely-used splitting protocol proposed by Ravi et al. [27], which uses 64 classes for meta-training, 16 classes for meta-validation, and 20 classes for meta-testing.

The **tieredImageNet dataset** is a larger subset of ImageNet, composed of 608 classes grouped into 34 high-level categories. They are further divided into 20 categories for meta-training, 6 categories for meta-validation, and 8 categories for meta-testing, which corresponds to 351, 97, and 160 classes for meta-training, meta-validation, and meta-testing, respectively. This splitting method, which considers high-level categories, is applied to minimize the semantic overlap between the splits. Images are of size 84×84 .

Results. Table 1 summarizes the results on the 5-way miniImageNet and tieredImageNet. Our method achieves state-of-the-art performance on the miniImageNet benchmark for both 5-way-1-shot and 5-way-5-shot tasks. On tieredImageNet, we also achieve the best performance on the 5-way-5-shot task and comparable performance on the 5-way-1-shot task. Note that related works use very complex training schemes to improve their performance. For example, LEO [30] used an encoder and relation network in addition to the WRN-28-10 backbone network to produce sample-depend initialization of the gradient descent. FEAT [39] and LEO [30] pre-train the WRN-28-10 backbone to classify 64 meta-training set of miniImageNet and then continue meta-training. TADAM [24] co-trained the feature embedding on both meta-training task (5-way) and the

Table 2. **Comparison to prior work on CIFAR-FS and FC100.** Average few-shot classification accuracies(%) with 95% confidence intervals on the meta-testing sets of CIFAR-FS and FC100. a-b-c-d denotes a 4-layer convolutional network with a, b, c, d filters in each layer.

model	backbone	CIFAR-FS 5-way		FC100 5-way	
		1-shot	5-shot	1-shot	5-shot
MAML [7]	32-32-32-32	58.9 \pm 1.9	71.5 \pm 1.0	-	-
Prototypical Networks [32]	64-64-64-64	55.5 \pm 0.7	72.0 \pm 0.6	35.3 \pm 0.6	48.6 \pm 0.6
Relation Networks [34]	64-96-128-256	55.0 \pm 1.0	69.3 \pm 0.8	-	-
R2D2 [1]	96-192-384-512	65.3 \pm 0.2	79.4 \pm 0.1	-	-
TADAM [24]	ResNet-12	-	-	40.1 \pm 0.4	56.1 \pm 0.4
Shot-Free [28]	ResNet-12	69.2 \pm n/a	84.7 \pm n/a	-	-
TEWAM [25]	ResNet-12	70.4 \pm n/a	81.3 \pm n/a	-	-
Prototypical Networks [32]	ResNet-12	72.2 \pm 0.7	83.5 \pm 0.5	37.5 \pm 0.6	52.5 \pm 0.6
MetaOptNet [18]	ResNet-12	72.6 \pm 0.7	84.3 \pm 0.5	41.1 \pm 0.6	55.5 \pm 0.6
RFS [35]	ResNet-12	73.9 \pm 0.8	86.9 \pm 0.5	44.6 \pm 0.7	60.9 \pm 0.6
MABAS [13]	ResNet-12	73.51 \pm 0.96	85.49 \pm 0.68	42.31 \pm 0.75	57.56 \pm 0.78
Ours	ResNet-12	74.13 \pm 0.71	87.54 \pm 0.51	44.82 \pm 0.73	61.31 \pm 0.54

Table 3. **Ablation study.** Performance of our ablated models on four few-shot classification benchmarks. The model is fixed when we conduct experiments about ablation for loss terms. The metric is average few-shot classification accuracies(%).

Attention	Cluster Loss	Sparse Loss	miniImageNet		tieredImageNet		CIFAR-FS		FC100	
			1-shot	5-shot	1-shot	5-shot	1-shot	5-shot	1-shot	5-shot
✓			60.31	77.73	70.26	82.11	70.09	83.32	40.02	57.10
✓	✓		61.03	79.44	71.10	83.42	71.67	84.59	41.13	58.25
✓	✓	✓	64.24	81.74	72.32	85.93	73.07	85.54	43.24	60.35
			65.74	83.03	73.82	86.76	74.13	87.54	44.82	61.31

standard classification task (64-way) together. FEAT [39] and MABAS [13] require additional fine-tuning on meta-testing sets. In contrast to all those approaches, our model just needs to train the embedding function through standard classification without further fine-tuning. This strategy allows us to clearly demonstrate the effect of a good embedding function by achieving stronger performance with an arguably simpler training. We also notice that when comparing to the best performance on each benchmark, the performance gain for miniImageNet is relatively larger than that of tieredImageNet.

4.3. Experiments on CIFAR derivatives

The CIFAR-FS dataset is a recently proposed few-shot image classification benchmark derived from CIFAR. It consists of all 100 classes and is further randomly split into 64 meta-training classes, 16 meta-validation classes, and 20 meta-testing classes. Each class contains 600 images of size 32×32 .

The FC100 dataset is another few-shot classification dataset based on CIFAR. Its main idea is very similar to tieredImageNet, where the whole 100 classes are grouped into 20 superclasses. Each superclass is composed of standard 5 classes. These superclasses are divided into 12, 4, 4 for meta-training, meta-validation, meta-testing correspondingly. Images are of size 32×32 pixels.

Results. Table 2 summarizes the performance on the 5-way CIFAR-FS and FC100. Our model achieves state-of-the-art performance on all tasks in both CIFAR-FS and FC100 benchmark. We observe that the relative improvement rate on the CIFAR-FS dataset is larger compared to the FC100 dataset which is similar to generalization pattern on the ImageNet derivatives. Namely, the performance on the benchmark with semantic gaps between the meta-training set and meta-testing set benefits less from our method. We expect to alleviate this problem by finding a good way to fine-tune our model at meta-testing stage in future work.

4.4. Ablation Experiments

In this section, we conduct ablation studies on our COM-PAS pipeline to analyze how its variants affect the few-shot classification result. We study the following three components of our method: (a) The attention module on activated spatial distribution maps; (b) The cluster loss of the part dictionary; (c) The sparse loss of the map dictionary. In addition, we also analyze the result of the number of components in the part dictionary D , map dictionary S .

Table 3 shows the result of our ablation studies on miniImageNet, tieredImageNet, CIFAR-FS and FC100. We can see that the attention mechanism for augmenting important parts and their relationship makes the average performance improve on average around 1.2% on all datasets. With our

Table 4. **Test accuracies(%) on meta-testing set of miniImageNet with a varying number of components in the part dictionary.** Either too much or too less components harm the performance of the model.

Part Dictionary Size B	miniImageNet	
	1-shot	5-shot
256	63.82	81.13
512	65.74	83.03
1024	65.12	82.45

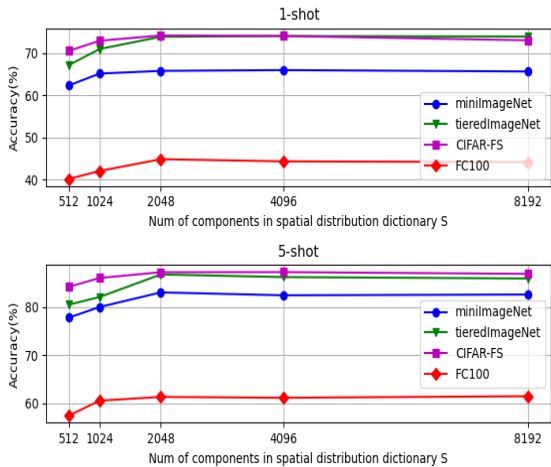


Figure 4. **Test accuracies(%) on meta-testing sets with a varying number of components in the map dictionary.** The performance of our model increases at first and saturates at some point with a slight tendency to drop for large numbers of components.

cluster loss that regularizes the components in the part dictionary D , we gain on average about 2.3%. In addition, this loss increases the interpretability of our model as it makes the image patches detected by these part detectors more semantically meaningful. Our sparse loss regularizer improves the performance by another 1.5%, which demonstrates the benefit of making the components in the map dictionary distinct from each other.

Table 4 shows the influence of the size B of the part dictionary D on the performance of our model on miniImageNet. With too less components in the dictionary, our model do not contain enough information for modeling the part-whole based relationships of the objects. However, if the size B becomes too large, it harms each part representation to accurately capture the corresponding features and many components might focus on meaningless background thus enlarge the learning difficulty.

Figure 4 illustrates the influence of the number of components in the map dictionary S on the performance of our model on four benchmarks. The performance improves at first when the number of components increases but saturates as the dictionaries become larger. The performance

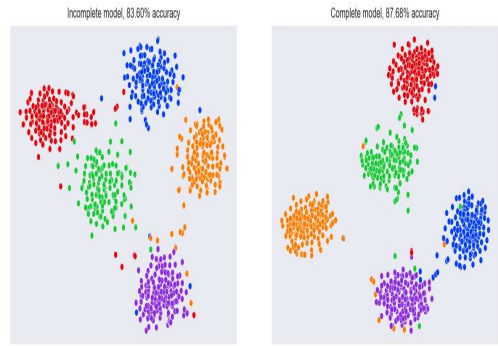


Figure 5. **t-SNE visualization illustrating improved feature embeddings with our designed modules.** The left figure corresponds to our model without attention module, cluster loss, and sparse loss. The right figure corresponds to the complete model.

keeps at the same level and even shows a tendency to drop. These results suggest that when the capacity of the dictionary is small, our model cannot store all necessary information. However, if the capacity becomes too large, the model starts to overfit slightly.

In Figure 5, we further show the t-SNE visualization results of the embedding space of our model on the CIFAR-FS dataset. For both t-SNE plots, we use the same data and the same hyper-parameters. The left figure shows the embedding space without using attention, the cluster, and sparse loss for regularization. The right figure shows the result with the full model. We can observe that even without these modules, the initial embedding is quite good which can be attributed to the novel architecture design. However, after adding these modules, the cluster centers are forced to become even denser and more distinct from each other.

5. Conclusion

In this work, we study the problem of few-shot image classification. Inspired by the compositional representation of objects in humans, we introduce COMPAS, a novel neural architecture for few-shot classification that learns through compositional part sharing. In particular, COMPAS learns a knowledge base that contains a dictionary of part representations and a dictionary of part activation maps that encode frequent spatial activation patterns of parts. During meta-testing, this knowledge is reused to learn about unseen classes from very few samples. Our extensive experiments demonstrate the effectiveness of our method, which achieves state-of-the-art performance on four popular few-shot classification benchmarks.

References

- [1] Luca Bertinetto, João F. Henriques, Philip H. S. Torr, and Andrea Vedaldi. Meta-learning with differentiable closed-form solvers, 2019. 2, 5, 6, 7
- [2] Jifeng Dai, Yi Hong, Wenze Hu, Song-Chun Zhu, and Ying Nian Wu. Unsupervised learning of dictionaries of hierarchical compositional models. In *Proceedings of the IEEE Conference on Computer Vision and Pattern Recognition (CVPR)*, June 2014. 3
- [3] Guneet S. Dhillon, Pratik Chaudhari, Avinash Ravichandran, and Stefano Soatto. A baseline for few-shot image classification, 2020. 5
- [4] Nikita Dvornik, Cordelia Schmid, and Julien Mairal. Diversity with cooperation: Ensemble methods for few-shot classification. In *Proceedings of the IEEE/CVF International Conference on Computer Vision*, pages 3723–3731, 2019. 6
- [5] Sanja Fidler, Marko Boben, and Ales Leonardis. Learning a hierarchical compositional shape vocabulary for multi-class object representation, 2014. 3
- [6] Sanja Fidler and Ales Leonardis. Towards scalable representations of object categories: Learning a hierarchy of parts. In *2007 IEEE Conference on Computer Vision and Pattern Recognition*, pages 1–8. IEEE, 2007. 3
- [7] Chelsea Finn, Pieter Abbeel, and Sergey Levine. Model-agnostic meta-learning for fast adaptation of deep networks, 2017. 1, 2, 6, 7
- [8] Mohammad Ghasemzadeh, Fang Lin, Bita Darvish Rouhani, Farinaz Koushanfar, and Ke Huang. Agilenet: Lightweight dictionary-based few-shot learning, 2018. 1
- [9] Spyros Gidaris and Nikos Komodakis. Dynamic few-shot visual learning without forgetting. In *Proceedings of the IEEE Conference on Computer Vision and Pattern Recognition (CVPR)*, June 2018. 1, 2, 6
- [10] Bharath Hariharan and Ross Girshick. Low-shot visual recognition by shrinking and hallucinating features. In *Proceedings of the IEEE International Conference on Computer Vision (ICCV)*, Oct 2017. 1
- [11] Kaiming He, Xiangyu Zhang, Shaoqing Ren, and Jian Sun. Deep residual learning for image recognition. In *Proceedings of the IEEE conference on computer vision and pattern recognition*, pages 770–778, 2016. 1, 2
- [12] Jie Hu, Li Shen, and Gang Sun. Squeeze-and-excitation networks. In *Proceedings of the IEEE Conference on Computer Vision and Pattern Recognition (CVPR)*, June 2018. 4
- [13] Jaekyeom Kim, Hyoungseok Kim, and Gunhee Kim. Model-agnostic boundary-adversarial sampling for test-time generalization in few-shot learning. 6, 7
- [14] Adam Kortylewski, Ju He, Qing Liu, and Alan L. Yuille. Compositional convolutional neural networks: A deep architecture with innate robustness to partial occlusion. In *Proceedings of the IEEE/CVF Conference on Computer Vision and Pattern Recognition (CVPR)*, June 2020. 3
- [15] Adam Kortylewski, Qing Liu, Angtian Wang, Yihong Sun, and Alan Yuille. Compositional convolutional neural networks: A robust and interpretable model for object recognition under occlusion. *International Journal of Computer Vision*, pages 1–25, 2020. 3
- [16] Adam Kortylewski, Qing Liu, Huiyu Wang, Zhishuai Zhang, and Alan Yuille. Combining compositional models and deep networks for robust object classification under occlusion. *arXiv preprint arXiv:1905.11826*, 2019. 3
- [17] Alex Krizhevsky, Ilya Sutskever, and Geoffrey E. Hinton. Imagenet classification with deep convolutional neural networks. In *Advances in neural information processing systems*, pages 1097–1105, 2012. 1
- [18] Kwonjoon Lee, Subhransu Maji, Avinash Ravichandran, and Stefano Soatto. Meta-learning with differentiable convex optimization. In *Proceedings of the IEEE/CVF Conference on Computer Vision and Pattern Recognition (CVPR)*, June 2019. 1, 2, 5, 6, 7
- [19] Renjie Liao, Alex Schwing, Richard Zemel, and Raquel Urtasun. Learning deep parsimonious representations. In *Advances in Neural Information Processing Systems*, pages 5076–5084, 2016. 2, 3
- [20] Bin Liu, Yue Cao, Yutong Lin, Qi Li, Zheng Zhang, Ming-sheng Long, and Han Hu. Negative margin matters: Understanding margin in few-shot classification, 2020. 6
- [21] Nikhil Mishra, Mostafa Rohaninejad, Xi Chen, and Pieter Abbeel. A simple neural attentive meta-learner, 2018. 5
- [22] Tsendsuren Munkhdalai, Xingdi Yuan, Soroush Mehri, and Adam Trischler. Rapid adaptation with conditionally shifted neurons. volume 80 of *Proceedings of Machine Learning Research*, pages 3664–3673, Stockholm, Sweden, 10–15 Jul 2018. PMLR. 6
- [23] Alex Nichol and John Schulman. Reptile: a scalable metalearning algorithm. *arXiv: Learning*, 2018. 1, 2
- [24] Boris Oreshkin, Pau Rodríguez López, and Alexandre Lacoste. Tadam: Task dependent adaptive metric for improved few-shot learning. In S. Bengio, H. Wallach, H. Larochelle, K. Grauman, N. Cesa-Bianchi, and R. Garnett, editors, *Advances in Neural Information Processing Systems*, volume 31, pages 721–731. Curran Associates, Inc., 2018. 1, 2, 5, 6, 7
- [25] Limeng Qiao, Yemin Shi, Jia Li, Yaowei Wang, Tiejun Huang, and Yonghong Tian. Transductive episodic-wise adaptive metric for few-shot learning. In *Proceedings of the IEEE/CVF International Conference on Computer Vision (ICCV)*, October 2019. 6, 7
- [26] Siyuan Qiao, Chenxi Liu, Wei Shen, and Alan L. Yuille. Few-shot image recognition by predicting parameters from activations. In *Proceedings of the IEEE Conference on Computer Vision and Pattern Recognition (CVPR)*, June 2018. 1, 2
- [27] Sachin Ravi and Hugo Larochelle. Optimization as a model for few-shot learning. 2016. 6
- [28] Avinash Ravichandran, Rahul Bhotika, and Stefano Soatto. Few-shot learning with embedded class models and shot-free meta training. In *Proceedings of the IEEE/CVF International Conference on Computer Vision (ICCV)*, October 2019. 5, 6, 7
- [29] Mengye Ren, Eleni Triantafillou, Sachin Ravi, Jake Snell, Kevin Swersky, Joshua B. Tenenbaum, Hugo Larochelle, and Richard S. Zemel. Meta-learning for semi-supervised few-shot classification, 2018. 2, 5

[30] Andrei A. Rusu, Dushyant Rao, Jakub Sygnowski, Oriol Vinyals, Razvan Pascanu, Simon Osindero, and Raia Hadsell. Meta-learning with latent embedding optimization, 2019. 6

[31] Karen Simonyan and Andrew Zisserman. Very deep convolutional networks for large-scale image recognition. *arXiv preprint arXiv:1409.1556*, 2014. 1

[32] Jake Snell, Kevin Swersky, and Richard Zemel. Prototypical networks for few-shot learning. In I. Guyon, U. V. Luxburg, S. Bengio, H. Wallach, R. Fergus, S. Vishwanathan, and R. Garnett, editors, *Advances in Neural Information Processing Systems*, volume 30, pages 4077–4087. Curran Associates, Inc., 2017. 1, 2, 6, 7

[33] Yihong Sun, Adam Kortylewski, and Alan Yuille. Weakly-supervised amodal instance segmentation with compositional priors, 2020. 3

[34] Flood Sung, Yongxin Yang, Li Zhang, Tao Xiang, Philip H.S. Torr, and Timothy M. Hospedales. Learning to compare: Relation network for few-shot learning. In *Proceedings of the IEEE Conference on Computer Vision and Pattern Recognition (CVPR)*, June 2018. 1, 2, 6, 7

[35] Yonglong Tian, Yue Wang, Dilip Krishnan, Joshua B. Tenenbaum, and Phillip Isola. Rethinking few-shot image classification: a good embedding is all you need?, 2020. 1, 2, 6, 7

[36] Oriol Vinyals, Charles Blundell, Timothy Lillicrap, koray kavukcuoglu, and Daan Wierstra. Matching networks for one shot learning. In D. Lee, M. Sugiyama, U. Luxburg, I. Guyon, and R. Garnett, editors, *Advances in Neural Information Processing Systems*, volume 29, pages 3630–3638. Curran Associates, Inc., 2016. 1, 2, 5, 6

[37] Fangyu Wu, Jeremy S. Smith, Wenjin Lu, Chaoyi Pang, and Bailing Zhang. Attentive prototype few-shot learning with capsule network-based embedding. In Andrea Vedaldi, Horst Bischof, Thomas Brox, and Jan-Michael Frahm, editors, *Computer Vision – ECCV 2020*, pages 237–253, Cham, 2020. Springer International Publishing. 3

[38] Ya Jin and S. Geman. Context and hierarchy in a probabilistic image model. In *2006 IEEE Computer Society Conference on Computer Vision and Pattern Recognition (CVPR'06)*, volume 2, pages 2145–2152, 2006. 3

[39] Han-Jia Ye, Hexiang Hu, De-Chuan Zhan, and Fei Sha. Few-shot learning via embedding adaptation with set-to-set functions. In *Proceedings of the IEEE/CVF Conference on Computer Vision and Pattern Recognition (CVPR)*, June 2020. 1, 2, 6, 7

[40] Jian Zhang, Chenglong Zhao, Bingbing Ni, Minghao Xu, and Xiaokang Yang. Variational few-shot learning. In *Proceedings of the IEEE/CVF International Conference on Computer Vision (ICCV)*, October 2019. 6

[41] Quanshi Zhang, Ying Nian Wu, and Song-Chun Zhu. Interpretable convolutional neural networks. In *Proceedings of the IEEE Conference on Computer Vision and Pattern Recognition (CVPR)*, June 2018. 2, 3

[42] Zhishuai Zhang, Cihang Xie, Jianyu Wang, Lingxi Xie, and Alan L Yuille. Deepvoting: A robust and explainable deep network for semantic part detection under partial occlusion. In *Proceedings of the IEEE Conference on Computer Vision and Pattern Recognition*, pages 1372–1380, 2018. 2

[43] Long Zhu, Yuanhao Chen, Antonio Torralba, William Freeman, and Alan Yuille. Part and appearance sharing: Recursive compositional models for multi-view. In *2010 IEEE Computer Society Conference on Computer Vision and Pattern Recognition*, pages 1919–1926. IEEE, 2010. 3

[44] Long (Leo) Zhu, Chenxi Lin, Haoda Huang, Yuanhao Chen, and Alan Yuille. Unsupervised structure learning: Hierarchical recursive composition, suspicious coincidence and competitive exclusion. In David Forsyth, Philip Torr, and Andrew Zisserman, editors, *Computer Vision – ECCV 2008*, pages 759–773, Berlin, Heidelberg, 2008. Springer Berlin Heidelberg. 3